atmosphere

MDPI

Article

Urban–Suburban $PM_{2.5}$ Trends in China Under Different Urban Classification Methods

Ning Yang [1,*], Yuanwei Zhong [1], Fengjuan Fan [1], Guangjin Liu [1], Zonghan Xue [1], Yanru Bai [2] and Nan Lu [1]

[1] College of Environment and Climate, Institute for Environmental and Climate Research, Guangdong-Hongkong-Macau Joint Laboratory of Collaborative Innovation for Environmental Quality, Jinan University, Guangzhou 510632, China; zhongyw2024@stu2024.jnu.edu.cn (Y.Z.); fanfj@stu2025.jnu.edu.cn (F.F.); liugj@stu2022.jnu.edu.cn (G.L.); xzh171618@stu2023.jnu.edu.cn (Z.X.); nanlu@stu2018.jnu.edu.cn (N.L.)

[2] Department of Ecological and Environmental Engineering, Shaanxi A&F Technology University, Shaanxi 712100, China; baiyanru@stu2018.jnu.edu.cn

* Correspondence: yangn@stu2020.jnu.edu.cn; Tel.: +86-15755460935

Abstract

Urban–suburban $PM_{2.5}$ differences are widely used to characterize spatial disparities in air pollution, yet their long-term trends may depend on urban definitions. For China during 2013–2020, this study used nationwide ground $PM_{2.5}$ monitoring data and 1 km × 1 km gridded population density data to analyze the sensitivity of urban–suburban $PM_{2.5}$ trends to spatial structure-based and population-density-based classification (300, 1500, 2200, 2500 people km^{-2}) at national, Eastern and Western China scales. Results showed significant national $PM_{2.5}$ decline, with urban reduction rates of −3.1 to −3.3 μg m^{-3} yr^{-1} in summer and −6.0 to −6.3 μg m^{-3} yr^{-1} in winter, and faster air quality improvement in winter. Urban–suburban $PM_{2.5}$ differences were highly sensitive to classification methods: the spatial structure-based framework showed minimal differences (0.09 μg m^{-3} in summer, 5 μg m^{-3} in winter), while the 300 people km^{-2} threshold yielded much larger ones (11 μg m^{-3} in summer, 29 μg m^{-3} in winter) with faster urban declines. Higher population density thresholds narrowed such differences and converged trends with the spatial structure-based results. Pronounced spatial heterogeneity existed: Eastern China had larger $PM_{2.5}$ declines with consistent response patterns to national trends, while Western China showed weaker declines, with urban–suburban differences highly sensitive to classification methods and opposite temporal evolution trends. This study confirms that urban definition is a critical methodological factor for interpreting China's long-term urban–suburban $PM_{2.5}$ trends, as different methods cause notable inferential deviations. Future air pollution spatial heterogeneity studies should carefully select and specify urban classification methods to ensure comparable, scientifically rigorous findings.

Keywords: $PM_{2.5}$; urban classification; urban–suburban differences; driving factors

Academic Editor: Kimitaka Kawamura

Received: 20 March 2026
Revised: 8 April 2026
Accepted: 14 April 2026
Published: 16 April 2026

1. Introduction

Fine particulate matter ($PM_{2.5}$) has been a major air quality concern in China over the past decade due to its significant impacts on public health and atmospheric visibility [1–4]. In response to severe $PM_{2.5}$ pollution, a series of stringent emission-control policies have been implemented, including the Air Pollution Prevention and Control Action Plan and the subsequent Blue Sky Protection Campaign [5,6]. These measures have led to substantial nationwide improvements in air quality during 2013–2020 [7,8]. However, most previous

studies have primarily focused on long-term $PM_{2.5}$ trends at national or regional scales, while comparatively little attention has been paid to long-term differences between urban and suburban areas across China. For example, several studies have examined nationwide trends in China during 2013–2023 [9–11], while others have investigated regional variations over longer periods such as 2000–2020 [12–14]. Some studies have also analyzed $PM_{2.5}$ trends across both national and regional scales for the period 2013–2020 [15,16].

Despite these advances, relatively little attention has been paid to long-term differences between urban and suburban areas, particularly at the national scale. Urban–suburban contrasts in $PM_{2.5}$ provide important insights into spatial heterogeneity in air pollution and the effectiveness of emission-control strategies. However, existing studies have reported inconsistent findings regarding the evolution of these contrasts. For instance, in the Yangtze River Delta (YRD), Zhang et al. [17] reported a narrowing urban–suburban $PM_{2.5}$ gap, whereas Liu et al. [18] found an expanding urban–suburban gap. A key source of these discrepancies lies in the different urban–suburban classification criteria based on population density: Zhang et al. [17] defined urban areas using a threshold of 300 people km^{-2}, whereas Liu et al. [18] adopted a stricter threshold of 2200 people km^{-2}. These differences further led to distinct interpretations of the relative decline rates of $PM_{2.5}$ concentrations in urban and suburban areas. Zhang et al. [17] attributed the narrowing gap to faster declines in urban $PM_{2.5}$ concentrations compared with suburban areas, and although Liu et al. [18] also reported faster declines in urban areas, their results indicated higher $PM_{2.5}$ concentrations in suburban areas than in urban sites, which contrasts with the concentration patterns reported by Zhang et al. [17]. Notably, at the national scale, several studies have suggested that the long-term urban–suburban difference in $PM_{2.5}$ concentrations has generally decreased over time [5,19,20]. These inconsistencies may partly arise from differences in methodological approaches. One important but often overlooked source of such methodological uncertainty lies in the definition of urban and suburban areas. Previous studies have adopted various approaches to classify urban–suburban regions, including urban spatial structure theories (e.g., concentric-zone or core–periphery models) [21] and population-density-based thresholds (e.g., 2500, 2200, 1500, or 300 people km^{-2}) [17–19,22]. Because these classification methods can produce substantially different spatial delineations of urban and suburban areas, the resulting estimates of urban–suburban $PM_{2.5}$ differences and their long-term trends may also vary. However, the sensitivity of urban–suburban $PM_{2.5}$ trend analyses to different urban classification methods has not been systematically evaluated.

To address this gap, this study systematically investigates the sensitivity of urban–suburban $PM_{2.5}$ differences and their long-term trends to different urban classification methods across China during 2013–2020. We compare the widely used urban–suburban framework based on urban spatial structure theories, such as the concentric-zone or core–periphery model proposed by Gao et al. [21], with population-density-based approaches using multiple density thresholds. Based on long-term surface observations, we quantify how different classification schemes influence the magnitude and temporal evolution of urban–suburban $PM_{2.5}$ contrasts at both national and regional scales. This work aims to provide a more robust understanding of urban–suburban $PM_{2.5}$ trends and to highlight the importance of consistent and physically meaningful urban definitions in air quality studies.

2. Materials and Methods

2.1. $PM_{2.5}$ Observations and Population Density Data

Daily $PM_{2.5}$ concentration data were obtained from the China National Environmental Monitoring Center (CNEMC; https://www.cnemc.cn/, accessed on 1 January 2021), covering the period from 1 January 2013 to 31 December 2020. The CNEMC network provides

nationwide observations from more than 1600 monitoring stations across mainland China and has been widely used in previous studies of long-term air-quality trends [19,20]. To ensure data quality, monitoring stations with annual missing rates greater than 20% were excluded from the analysis. After this quality control procedure, the number of valid monitoring stations for the period 2013–2020 was 403, 903, 1450, 1433, 1457, 1475, 1449, and 1436, respectively.

Gridded population data with a spatial resolution of 1 km × 1 km were obtained from the Resource and Environment Science and Data Center (RESDC; https://www.resdc.cn/, accessed on 15 January 2021). Population density is widely used as an indicator of urban spatial structure, as it reflects the intensity of human activities and the spatial distribution of urban development [23]. In this study, the 2015 population dataset, a typical year within the 2013–2020 study period, was used as the reference for urban–suburban classification. Each monitoring station was assigned a population density value extracted from the corresponding grid cell of the population dataset. This information was then used to classify stations into urban and suburban categories under different population density thresholds.

2.2. Urban–Suburban Classification Methods

To evaluate the sensitivity of urban–suburban $PM_{2.5}$ differences to urban definitions, two types of classification frameworks were considered in this study. First, we adopted the widely used urban–suburban classification proposed by Gao et al. [21], which is based on urban spatial structure theories such as concentric-zone or core–periphery models. In this framework, monitoring stations are categorized according to their relative locations within the urban spatial structure. Second, we applied population-density-based classification methods using multiple density thresholds. Previous studies have suggested a range of population density thresholds for defining urban areas in China, including 300, 1500, 2200, and 2500 people km^{-2} [17–19,22]. To assess the influence of these thresholds on urban–suburban classification, we applied each threshold to the gridded population dataset. Monitoring stations located in grid cells with population density exceeding the selected threshold were classified as urban stations, while the remaining stations were categorized as suburban stations. Figure 1 shows the spatial distribution of monitoring stations classified as urban and suburban using (a) the method of Gao et al. [21] and population density thresholds of (b) 300, (c) 1500, (d) 2200, and (e) 2500 people km^{-2}.

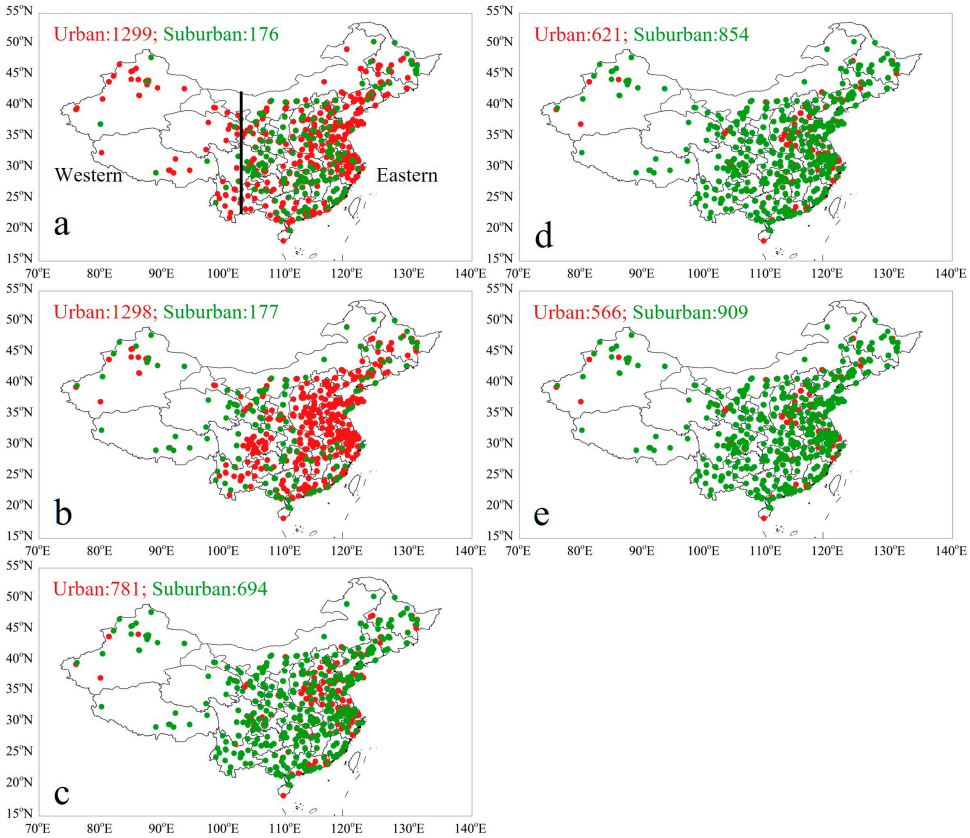

Figure 1. Spatial distribution of monitoring stations classified as urban and suburban across mainland China and subregions (Eastern and Western) under different classification methods. Urban stations are shown in red and suburban stations in green. Panel (**a**) shows the classification based on the urban spatial structure framework proposed by Gao et al. [21]. Panels (**b**–**e**) present classifications based on population density thresholds of 300, 1500, 2200, and 2500 people km^{-2}, respectively [17–19,22]. The number of urban and suburban stations under each classification scheme is indicated in each panel.

3. Results and Discussion

3.1. National Urban–Suburban $PM_{2.5}$ Trends and Their Sensitivity to Urban Classification Methods

Figure 2 illustrates the long-term trends of summer and winter $PM_{2.5}$ concentrations across China during 2013–2020 under different urban–suburban classification methods. Overall, $PM_{2.5}$ concentrations decreased substantially during the study period in both seasons, reflecting the nationwide improvements in air quality following the implementation of stringent emission-control policies [24–26]. In summer, national mean $PM_{2.5}$ concentrations exhibited a consistent downward trend across all classification methods. The decline rates ranged from −3.1 to −3.3 μg m^{-3} yr^{-1} for urban stations and from −1.3 to −3.9 μg m^{-3} yr^{-1} for suburban stations, depending on the classification approach. In winter, $PM_{2.5}$ concentrations were considerably higher but declined more rapidly than in summer, with urban trends ranging from −6.0 to −6.3 μg m^{-3} yr^{-1} and suburban trends ranging from −2.8 to −7.0 μg m^{-3} yr^{-1}. These results indicate that wintertime air quality improved more rapidly than summertime conditions across China.

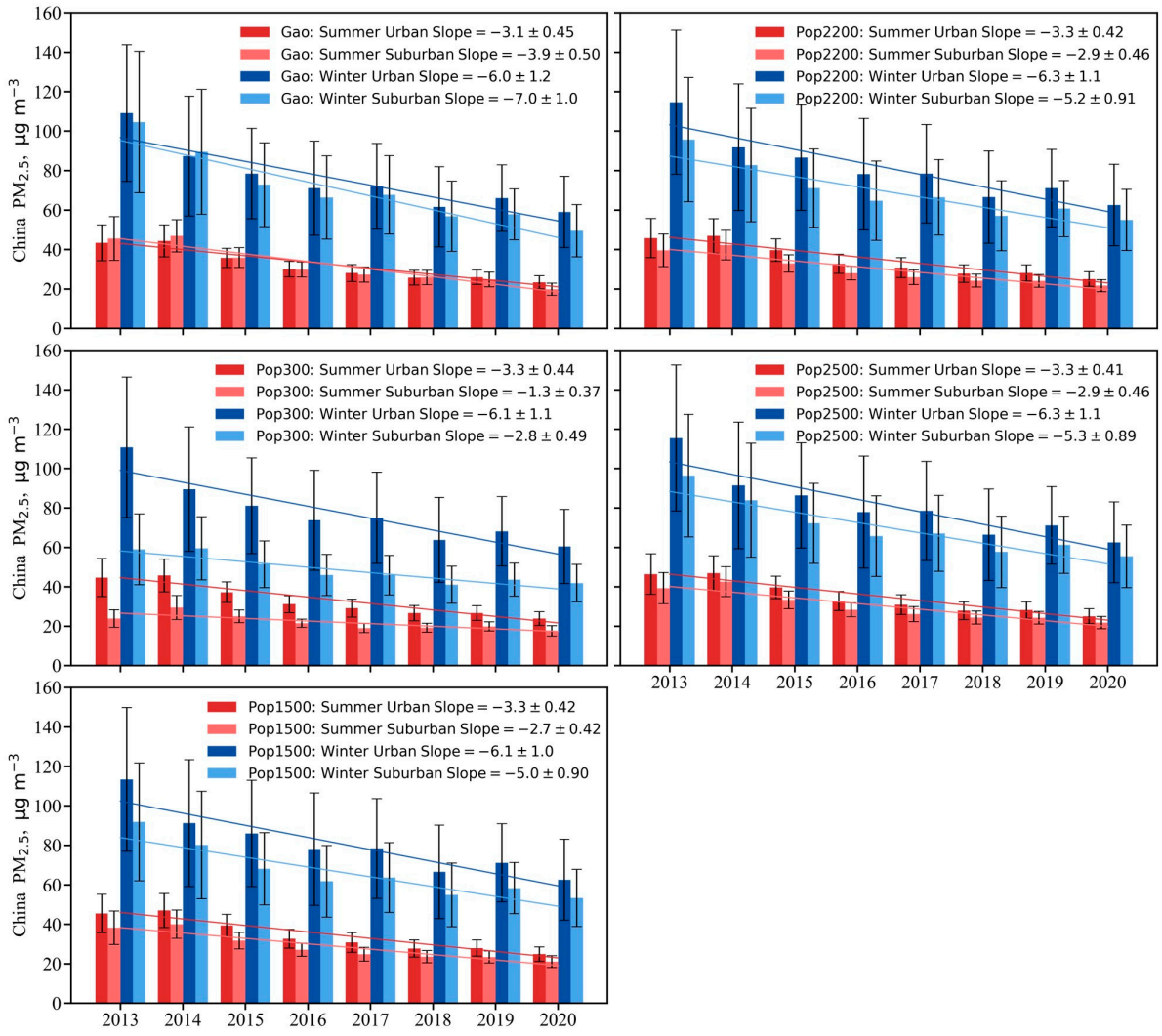

Figure 2. Observed trends in summer and winter $PM_{2.5}$ concentrations at urban and suburban monitoring sites across China from 2013 to 2020. Urban–suburban classifications are based on four different methods: the approach of Gao et al. [21] and population density thresholds of 300, 1500, 2200, and 2500 people km^{-2} (Pop300, Pop1500, Pop2200, and Pop2500). Bar charts represent the mean $PM_{2.5}$ concentrations, with error bars indicating the sample standard deviation of daily observations. Linear regression lines are fitted for the 2013–2020 period; the slopes are reported as the mean value $PM_{2.5}$ one standard deviation of the fit.

Despite the overall decreasing trends, the relative decline rates between urban and suburban areas varied substantially depending on the classification method. Under the urban spatial structure framework proposed by Gao et al. [21], suburban $PM_{2.5}$ concentrations declined slightly faster than urban concentrations in both seasons. Specifically, summer $PM_{2.5}$ decreased at rates of -3.1 μg m^{-3} yr^{-1} in urban areas and -3.9 μg m^{-3} yr^{-1} in suburban areas, while winter $PM_{2.5}$ declined at -6.0 and -7.0 μg m^{-3} yr^{-1}, respectively. Consistent with these trends, the urban–suburban $PM_{2.5}$ difference in summer decreased during 2013–2017 and increased slightly afterward, although the overall difference remained negligible (mean: 0.090 μg m^{-3}). In contrast, the wintertime difference increased gradually during 2013–2020, with a mean value of about 5.0 μg m^{-3}. By comparison, the population-density-based classification using a threshold of 300 people km^{-2} yields markedly different results. Under this definition, urban $PM_{2.5}$ concentrations declined substantially faster than suburban concentrations. In summer, the urban decline rate reached -3.3 μg m^{-3} yr^{-1}, whereas the suburban decline rate was only -1.3 μg m^{-3} yr^{-1}.

A similar pattern was observed in winter, with urban and suburban trends of −6.1 and −2.8 μg m^{-3} yr^{-1}, respectively. Consistent with these trends, the urban–suburban $PM_{2.5}$ difference decreased steadily from 2013 to 2020, with mean differences of approximately 11 μg m^{-3} in summer and 29 μg m^{-3} in winter.

The contrasting results between the Gao classification and the Pop300 approach may be related to differences in the spatial distribution of stations classified as urban or suburban. As shown in Figure 1, although the total numbers of urban and suburban stations are similar under the two methods, substantial regional differences exist. In western China, where urban development is relatively limited, some stations classified as urban under the Gao framework are categorized as suburban when using the Pop300 threshold. In contrast, in eastern China, where urbanization has progressed rapidly, several stations classified as suburban under the Gao method are reclassified as urban under the population-density approach [23,27]. This spatial redistribution is broadly consistent with the rapid urbanization processes observed in China over the past decade [5,28]. In addition, emission-control policies in China have often prioritized pollution mitigation in urban centers, which may contribute to faster reductions in $PM_{2.5}$ concentrations at urban sites compared with suburban locations [29,30]. Consequently, the urban–suburban trends derived from the Pop300 classification are broadly consistent with findings reported in several previous studies [17,18,31]. These results suggest that Pop300 definitions may capture certain aspects of contemporary urban development in China.

As the population density threshold increases, the inferred urban–suburban trends become progressively closer to those derived from the Gao classification. When the threshold is set to 1500 people km^{-2}, suburban $PM_{2.5}$ concentrations decline more rapidly than under the 300 people km^{-2} threshold, reaching −2.7 μg m^{-3} yr^{-1} in summer and −5.0 μg m^{-3} yr^{-1} in winter. Correspondingly, the urban–suburban $PM_{2.5}$ difference decreases gradually during 2013–2020, with mean differences of approximately 5.7 μg m^{-3} in summer and 14 μg m^{-3} in winter. With a further rise in the threshold to 2200 people km^{-2}, the suburban trends (−2.9 μg m^{-3} yr^{-1} in summer and −5.2 μg m^{-3} yr^{-1} in winter) become even closer to those derived from the Gao framework. Under this definition, the urban–suburban $PM_{2.5}$ difference continues to decrease during 2013–2020, with mean differences of approximately 4.8 μg m^{-3} in summer and 12 μg m^{-3} in winter. Notably, the results at a threshold of 2500 people km^{-2} are similar to those at 2200 people km^{-2}. The suburban trends (−2.9 μg m^{-3} yr^{-1} in summer and −5.3 μg m^{-3} yr^{-1} in winter) become even closer to those derived from the Gao framework. Under this definition, the urban–suburban $PM_{2.5}$ difference continues to decrease during 2013–2020, with mean differences of approximately 4.7 μg m^{-3} in summer and 11 μg m^{-3} in winter. However, as shown in Figure 1, the Pop1500, Pop2200, and Pop2500 classifications assign a considerable number of stations within major urban agglomerations in eastern China to the suburban category. Such classifications may not fully reflect the present urban–suburban structure of these rapidly developed regions. This result suggests that excessively high population density thresholds may also influence the delineation of urban and suburban stations.

Overall, these results demonstrate that the magnitude and temporal evolution of urban–suburban $PM_{2.5}$ differences are highly sensitive to the definition of urban areas used in the analysis. The Gao classification suggests relatively small urban–suburban contrasts, whereas the population-density-based classification with a threshold of 300 people km^{-2} yields substantially larger differences and indicates faster declines in urban $PM_{2.5}$ concentrations than in suburban areas. Increasing the population density threshold (e.g., Pop1500, Pop2200, and Pop2500) shifts the resulting urban–suburban $PM_{2.5}$ trends toward those from the Gao classification but also reclassifies numerous stations in developed urban agglomerations as suburban, which may alter the representativeness

of the resulting spatial patterns. These findings highlight both the strong sensitivity of estimated urban–suburban $PM_{2.5}$ dynamics to the choice of urban classification scheme and the critical role of urban definitions in interpreting long-term $PM_{2.5}$ trends across China.

3.2. Regional Heterogeneity of Urban–Suburban $PM_{2.5}$ Trends in Eastern and Western China

Figure 3 shows the long-term trends of summer and winter $PM_{2.5}$ concentrations across eastern China during 2013–2020 under different urban–suburban classification methods. Overall, the temporal patterns in eastern China are broadly consistent with those observed at the national scale but exhibit slightly stronger declines, particularly in winter. For example, depending on the urban–suburban classification scheme used, summer urban $PM_{2.5}$ concentrations decrease at rates ranging from -3.2 to -3.4 μg m^{-3} yr^{-1}, while winter concentrations decrease even more markedly, with rates spanning -6.2 to -6.7 μg m^{-3} yr^{-1}. These values are comparable to or slightly stronger than the national trends and reflect the substantial improvement in air quality in eastern China during the past decade. Such rapid reductions are consistent with the intensive emission-control policies implemented in major urban agglomerations, including industrial emission reductions, residential heating controls, and transportation regulations [7,8,17,31].

Despite the similar overall trends, the inferred urban–suburban contrasts remain sensitive to the classification method. Under the Gao framework, suburban $PM_{2.5}$ concentrations decline slightly faster than urban concentrations, with summer and winter trends of -4.0 and -7.4 μg m^{-3} yr^{-1}, respectively. In contrast, the population-density-based Pop300 definition yields substantially slower suburban declines (-1.2 μg m^{-3} yr^{-1} in summer and -2.6 μg m^{-3} yr^{-1} in winter), leading to much larger urban–suburban differences. This discrepancy highlights the strong influence of classification criteria on the inferred trends.

As the population density threshold increases, the suburban trends gradually approach those derived from the Gao classification. For example, the suburban decline rate increases from -1.2 μg m^{-3} yr^{-1} under Pop300 to -2.8 μg m^{-3} yr^{-1} under Pop1500, -3.0 μg m^{-3} yr^{-1} under Pop2200, and -3.0 μg m^{-3} yr^{-1} under Pop2500 in summer, while winter trends increase from -2.6 to -5.1, -5.3, and -5.4 μg m^{-3} yr^{-1}, respectively. This progressive convergence suggests that higher population density thresholds tend to reclassify some densely populated suburban stations as urban sites. However, excessively high thresholds also shift many stations located within major urban agglomerations into the suburban category, which may not fully represent the current urban spatial structure of eastern China. Together, these results illustrate that varying population density thresholds can substantially alter the delineation of urban and suburban stations, and in turn exert a marked influence on the estimated urban–suburban $PM_{2.5}$ trends in this region.

Figure 3 also shows the long-term trends of summer and winter $PM_{2.5}$ concentrations across western China during 2013–2020 under different urban–suburban classification methods. Interestingly, the trends in western China differ substantially from those observed at the national scale and in eastern China. The reduction in $PM_{2.5}$ concentrations during 2013–2020 is considerably weaker in western China. In summer, urban $PM_{2.5}$ concentrations decline at rates ranging from -0.79 μg m^{-3} yr^{-1} (Pop1500) to -1.4 μg m^{-3} yr^{-1} (Gao classification), which are substantially smaller than the corresponding declines observed nationally (approximately -3.1 to -3.3 μg m^{-3} yr^{-1}) and in eastern China (-3.2 to -3.4 μg m^{-3} yr^{-1}). Wintertime trends show an even stronger contrast. Urban $PM_{2.5}$ concentrations decline at rates ranging from -1.6 μg m^{-3} yr^{-1} (Gao classification) to 2.5 μg m^{-3} yr^{-1} (Pop2500), which are substantially smaller than the corresponding declines observed nationally (approximately -6.0 to -6.3 μg m^{-3} yr^{-1}) and in eastern China (-6.2 to -6.7 μg m^{-3} yr^{-1}).

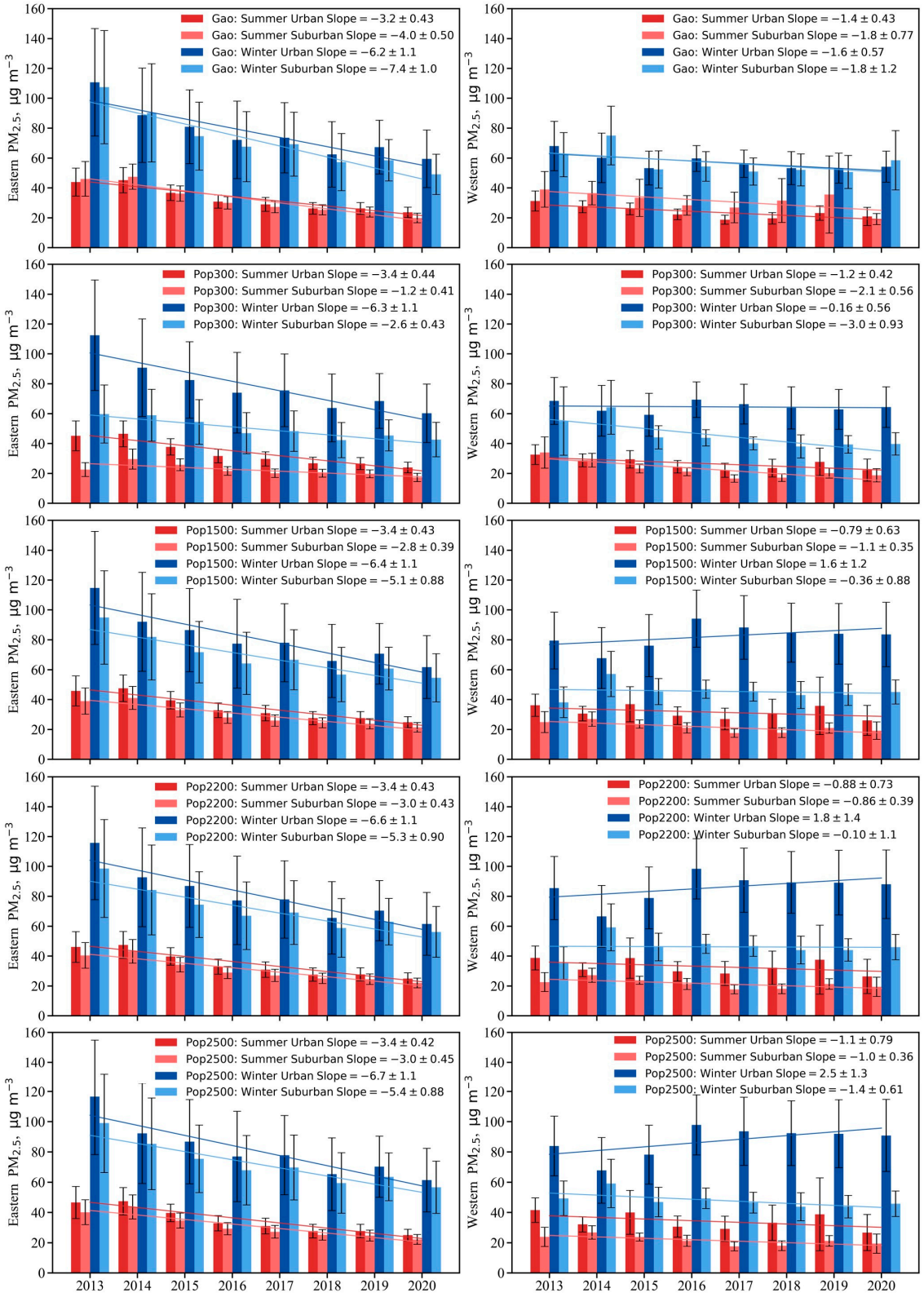

Figure 3. Observed trends in summer and winter $PM_{2.5}$ concentrations at urban and suburban monitoring sites across eastern and western China from 2013 to 2020.

Another notable feature is the strong dependence of the inferred trends on the classification method. Under the population-density-based definitions, winter urban trends vary substantially as the threshold increases. For example, the urban winter trend changes from -0.16 μg m^{-3} yr^{-1} under the Pop300 classification to positive values of 1.6 μg m^{-3} yr^{-1}

(Pop1500), positive values of 1.8 μg m^{-3} yr^{-1} (Pop2200), and 2.5 μg m^{-3} yr^{-1} (Pop2500). In contrast, suburban $PM_{2.5}$ concentrations generally continue to decrease, with trends of −0.10 μg m^{-3} yr^{-1} under Pop2200 and −3.0 μg m^{-3} yr^{-1} under Pop300. These results indicate that the inferred urban–suburban differences in western China are highly sensitive to the classification approach and can even change sign depending on the population density threshold. As a consequence, the urban–suburban $PM_{2.5}$ differences in western China exhibit a different temporal evolution from those observed at the national scale and in eastern China. For example, under the Pop300 classification, the urban–suburban contrast in western China gradually increases during 2013–2020 in both summer and winter, whereas the corresponding differences at the national scale and in eastern China show a clear decreasing trend.

The weaker and more variable trends in western China likely reflect several regional characteristics. Compared with eastern China, western regions have lower population densities, fewer monitoring stations, and weaker urban–suburban gradients, which increases the sensitivity of station classification to population density thresholds. In addition, $PM_{2.5}$ concentrations in western China are more strongly influenced by natural sources such as dust emissions, arid climatic conditions, and complex topography. These factors can increase interannual variability and partially obscure long-term emission-driven trends. Furthermore, major national air-pollution control policies have historically focused on heavily polluted regions in eastern China, which may also contribute to the relatively modest $PM_{2.5}$ reductions observed in western regions.

4. Conclusions

This study systematically evaluates the sensitivity of urban–suburban $PM_{2.5}$ trends to different urban classification methods across China from 2013 to 2020 at national and regional scales and confirms a core methodological conclusion that urban definition is a critical factor for interpreting urban–suburban $PM_{2.5}$ disparities. Despite the consistent and substantial nationwide decline in $PM_{2.5}$ concentrations driven by stringent air pollution control policies—with urban winter reduction rates (−6.0 to −6.3 μg m^{-3} yr^{-1}) notably outpacing summer rates (−3.1 to −3.3 μg m^{-3} yr^{-1})—different classification approaches lead to significant inferential deviations in the magnitude and temporal evolution of urban–suburban $PM_{2.5}$ differences.

Urban–suburban $PM_{2.5}$ differences exhibit strong sensitivity to the selected classification framework: the spatial structure-based method yields minimal urban–suburban disparities (0.09 μg m^{-3} in summer, 5 μg m^{-3} in winter), while the population-density-based classification with a 300 people km^{-2} threshold results in far larger differences (11 μg m^{-3} in summer, 29 μg m^{-3} in winter) and a distinct pattern of faster urban $PM_{2.5}$ declines. Raising the population density threshold (1500, 2200, 2500 people km^{-2}) gradually narrows these disparities and converges the derived trends with the spatial structure-based results, yet excessively high thresholds reclassify numerous monitoring stations in Eastern China's major urban agglomerations as suburban, undermining the representativeness of classification for actual urban–suburban spatial structures.

Pronounced spatial heterogeneity exists in the sensitivity of urban–suburban $PM_{2.5}$ trends to classification methods across Eastern and Western China. Eastern China sees stronger $PM_{2.5}$ declines than the national average, with urban–suburban trend characteristics and their responses to different classification methods highly consistent with national patterns, a direct reflection of the intensive implementation of air pollution control policies in this region. In contrast, Western China shows markedly weaker $PM_{2.5}$ reduction trends, with urban summer decline rates as low as −0.79 to −1.4 μg m^{-3} yr^{-1}; its urban–suburban $PM_{2.5}$ differences are even more sensitive to classification methods, with the sign of such

disparities changing with adjusted density thresholds, a phenomenon linked to the region's low population density, strong natural source interference on $PM_{2.5}$ concentrations, and relatively limited policy implementation intensity.

This study finds that inconsistent urban–suburban delineation reduces the comparability of research findings on urban–suburban air quality and impairs the scientific rigor of subsequent analyses of pollution drivers and policy effectiveness, thus emphasizing the need to carefully select urban–suburban delineation methods in light of research scales and regional characteristics and clearly specify the delineation criteria in relevant studies; For future research, two directions are proposed: optimizing population density thresholds based on the unique geographical and urbanization characteristics of Western China to establish a region-adapted urban–suburban delineation system, analyzing the impact of urban–suburban delineation methods on the evaluation of air pollution control policy effects to support the formulation of differentiated urban–suburban pollution mitigation strategies.

Author Contributions: Conceptualization, methodology, writing—original draft preparation, and writing—review and editing, N.Y.; validation, Y.Z.; formal analysis, F.F.; investigation, G.L.; resources, Z.X.; data curation, Y.B. and N.L. All authors have read and agreed to the published version of the manuscript.

Funding: This research was funded by the Science and Technology Innovation Strategy of Guangdong Province (2019B121205004).

Institutional Review Board Statement: Not applicable.

Informed Consent Statement: Not applicable.

Data Availability Statement: The original contributions presented in this study are included in the article. Further inquiries can be directed to the corresponding author.

Acknowledgments: The authors acknowledge the support of the Science and Technology Innovation Strategy of Guangdong Province (2019B121205004).

Conflicts of Interest: The authors declare no conflicts of interest.

References

1. Zhang, R.H.; Zhu, S.Q.; Zhang, Z.L.; Zhang, H.R.; Tian, C.F.; Wang, S.; Wang, P.; Zhang, H.L. Long-term variations of air pollutants and public exposure in China during 2000–2020. *Sci. Total. Environ.* **2024**, *930*, 172606. [CrossRef] [PubMed]
2. Wang, C.; Wang, Y.; Shi, Z.; Sun, J.; Gong, K.; Li, J.; Qin, M.; Wei, J.; Li, T.; Kan, H.; et al. Effects of using different exposure data to estimate changes in premature mortality attributable to $PM_{2.5}$ and O_3 in China. *Environ. Pollut.* **2021**, *285*, 117242. [CrossRef] [PubMed]
3. Zhao, B.; Zheng, H.; Wang, S.; Smith, K.R.; Lu, X.; Aunan, K.; Gu, Y.; Wang, Y.; Ding, D.; Xing, J. Change in household fuels dominates the decrease in $PM_{2.5}$ exposure and premature mortality in China in 2005–2015. *Proc. Natl. Acad. Sci. USA* **2018**, *115*, 12401–12406. [CrossRef] [PubMed]
4. Li, K.; Jacob, D.J.; Liao, H.; Zhu, J.; Shah, V.; Shen, L.; Bates, K.H.; Zhang, Q.; Zhai, S. A two-pollutant strategy for improving ozone and particulate air quality in China. *Nat. Geosci.* **2019**, *12*, 906–910. [CrossRef]
5. Guo, L.; Wang, X.; Baklanov, A.; Shao, M. $PM_{2.5}$ Concentration Gap Reduction between Typical Urban and Nonurban China from 2000 to 2023. *ACS ES T Air* **2024**, *2*, 90–98. [CrossRef]
6. Wen, Z.; Ma, X.; Xu, W.; Si, R.; Liu, L.; Ma, M.; Zhao, Y.; Tang, A.; Zhang, Y.; Wang, K.; et al. Combined short-term and long-term emission controls improve air quality sustainably in China. *Nat. Commun.* **2024**, *15*, 5169. [CrossRef]
7. Geng, G.; Liu, Y.; Liu, Y.; Liu, S.; Cheng, J.; Yan, L.; Wu, N.; Hu, H.; Tong, D.; Zheng, B.; et al. Efficacy of China's clean air actions to tackle $PM_{2.5}$ pollution between 2013 and 2020. *Nat. Geosci.* **2024**, *17*, 987–994. [CrossRef]
8. Zhang, Q.; Zheng, Y.; Tong, D.; Shao, M.; Wang, S.; Zhang, Y.; Xu, X.; Wang, J.; He, H.; Liu, W.; et al. Drivers of improved $PM_{2.5}$ air quality in China from 2013 to 2017. *Proc. Natl. Acad. Sci. USA* **2019**, *116*, 24463–24469. [CrossRef]
9. Wang, F.Y.; Han, X.; Xie, H.; Gao, Y.; Guan, X.; Zhang, M.G. Investigating trends and causes of simultaneous high pollution from $PM_{2.5}$ and ozone in China, 2015–2023. *Atmos. Pollut. Res.* **2025**, *16*, 102351. [CrossRef]

10. Liu, X.; Yi, G.; Zhou, X.; Zhang, T.; Bie, X.; Li, J.; Tan, H. Spatio-temporal variations of $PM_{2.5}$ and O_3 in China during 2013-2021: Impact factor analysis. *Environ. Pollut.* **2023**, *334*, 122189. [CrossRef]
11. Xiao, Q.; Geng, G.; Xue, T.; Liu, S.; Cai, C.; He, K.; Zhang, Q. Tracking $PM_{2.5}$ and O_3 pollution and the related health burden in China 2013–2020. *Environ. Sci. Technol.* **2021**, *56*, 6922–6932. [CrossRef]
12. Dai, H.B.; Liao, H.; Li, K.; Yue, X.; Yang, Y.; Zhu, J.; Jin, J.B.; Li, B.J.; Jiang, X.W. Composited analyses of the chemical and physical characteristics of co-polluted days by ozone and $PM_{2.5}$ over 2013–2020 in the Beijing-Tianjin-Hebei region. *Atmos. Chem. Phys.* **2023**, *23*, 23–39. [CrossRef]
13. Dai, H.B.; Zhu, J.; Liao, H.; Li, J.D.; Liang, M.X.; Yang, Y.; Yue, X. Co-occurrence of ozone and $PM_{2.5}$ pollution in the Yangtze River Delta over 2013–2019: Spatiotemporal distribution and meteorological conditions. *Atmos. Res.* **2021**, *249*, 105363. [CrossRef]
14. Yan, F.; Chen, W.; Jia, S.; Zhong, B.; Yang, L.; Mao, J.; Chang, M.; Shao, M.; Yuan, B.; Situ, S.; et al. Stabilization for the secondary species contribution to $PM_{2.5}$ in the Pearl River Delta (PRD) over the past decade, China: A meta-analysis. *Atmos. Environ.* **2020**, *242*, 117817. [CrossRef]
15. Shao, T.; Wang, P.; Yu, W.; Gao, Y.; Zhu, S.; Zhang, Y.; Hu, D.; Zhang, B.; Zhang, H. Drivers of alleviated $PM_{2.5}$ and O_3 concentrations in China from 2013 to 2020. *Resour. Conserv. Recycl.* **2023**, *197*, 107110. [CrossRef]
16. Wang, Y.H.; Gao, W.K.; Wang, S.; Song, T.; Gong, Z.Y.; Ji, D.S.; Wang, L.L.; Liu, Z.R.; Tang, G.Q.; Huo, Y.F.; et al. Contrasting trends of $PM_{2.5}$ and surface-ozone concentrations in China from 2013 to 2017. *Natl. Sci. Rev.* **2020**, *7*, 1331–1339. [CrossRef]
17. Zhang, L.; Zhao, N.; Zhang, W.; Wilson, J.P. Changes in long-term $PM_{2.5}$ pollution in the urban and suburban areas of China's three largest urban agglomerations from 2000 to 2020. *Remote Sens.* **2022**, *14*, 1716. [CrossRef]
18. Liu, B.; Wang, L.; Zhang, L.; Bai, K.; Chen, X.; Zhao, G.; Yin, H.; Chen, N.; Li, R.; Xin, J.; et al. Evaluating urban and nonurban $PM_{2.5}$ variability under clean air actions in China during 2010–2022 based on a new high-quality dataset. *Int. J. Digit. Earth* **2024**, *17*, 2310734. [CrossRef]
19. Xing, L.; Mao, X.; Duan, K. Impacts of urban–rural disparities in the trends of $PM_{2.5}$ and ozone levels in China during 2013–2019. *Atmos. Pollut. Res.* **2022**, *13*, 101590. [CrossRef]
20. Xiao, Q.; Geng, G.; Liang, F.; Wang, X.; Lv, Z.; Lei, Y.; Huang, X.; Zhang, Q.; Liu, Y.; He, K. Changes in spatial patterns of $PM_{2.5}$ pollution in China 2000–2018: Impact of clean air policies. *Environ. Int.* **2020**, *141*, 105776. [CrossRef]
21. Gao, L.; Yue, X.; Meng, X.; Du, L.; Lei, Y.; Tian, C.; Qiu, L. Comparison of ozone and $PM_{2.5}$ concentrations over urban, suburban, and background sites in China. *Adv. Atmos. Sci.* **2020**, *37*, 1297–1309. [CrossRef]
22. Wang, W.; Parrish, D.D.; Wang, S.; Bao, F.; Ni, R.; Li, X.; Yang, S.; Wang, H.; Cheng, Y.; Su, H. Long-term trend of ozone pollution in China during 2014–2020: Distinct seasonal and spatial characteristics and ozone sensitivity. *Atmos. Chem. Phys.* **2022**, *22*, 8935–8949. [CrossRef]
23. Wang, H.; Yu, X.; Luo, L.; Li, R. Urban–Rural Boundary Delineation Based on Population Spatialization: A Case Study of Guizhou Province, China. *Sustainability* **2024**, *16*, 1787. [CrossRef]
24. Kong, L.; Tang, X.; Zhu, J.; Wang, Z.; Liu, B.; Zhu, Y.; Zhu, L.; Chen, D.; Hu, K.; Wu, H.; et al. High-resolution simulation dataset of hourly $PM_{2.5}$ chemical composition in China (CAQRA-aerosol) from 2013 to 2020. *Adv. Atmos. Sci.* **2025**, *42*, 697–712. [CrossRef]
25. Niu, L.; Zhang, Z.F.; Liang, Y.Z.; van Vliet, J. Spatiotemporal patterns and drivers of the urban air pollution island effect for 2273 cities in China. *Environ. Int.* **2024**, *184*, 108455. [CrossRef]
26. Liu, S.G.; Geng, G.N.; Xiao, Q.Y.; Zheng, Y.X.; Liu, X.D.; Cheng, J.; Zhang, Q. Tracking Daily Concentrations of $PM_{2.5}$ Chemical Composition in China since 2000. *Environ. Sci. Technol.* **2022**, *56*, 16517–16527. [CrossRef]
27. Zhao, M.; Cheng, C.; Zhou, Y.; Li, X.; Shen, S.; Song, C. A global dataset of annual urban extents (1992–2020) from harmonized nighttime lights. *Earth Syst. Sci. Data* **2021**, *14*, 517–534. [CrossRef]
28. Liu, Y.; Geng, G.; Cheng, J.; Liu, Y.; Xiao, Q.; Liu, L.; Shi, Q.; Tong, D.; He, K.; Zhang, Q. Drivers of increasing ozone during the two phases of clean air actions in China 2013–2020. *Environ. Sci. Technol.* **2023**, *57*, 8954–8964. [CrossRef]
29. Zhu, S.; Liu, Z.; He, C. China's high-speed rail widens urban–rural disparities in air pollution and public health. *Nat. Cities* **2026**, *3*, 347–358. [CrossRef]
30. Song, Z.; Chen, B. Urban-rural patterns and driving factors of particulate matter pollution decrease in eastern China. *Atmos. Chem. Phys.* **2025**, *25*, 15487–15506. [CrossRef]
31. Dai, H.; Liao, H.; Wang, Y.; Qian, J. Co-occurrence of ozone and $PM_{2.5}$ pollution in urban/non-urban areas in eastern China from 2013 to 2020: Roles of meteorology and anthropogenic emissions. *Sci. Total. Environ.* **2024**, *924*, 171687. [CrossRef]